The Cryosphere Discuss., 9, 6545–6579, 2015
www.the-cryosphere-discuss.net/9/6545/2015/
doi:10.5194/tcd-9-6545-2015

The Cryosphere Discussions
Open Access

Modeling Antarctic subglacial lake filling and drainage cycles

C. F. Dow[1], M. A. Werder[2], S. Nowicki[1], and R. T. Walker[1,3]

[1]Cryopheric Sciences Laboratory, NASA Goddard Space Flight Center, Greenbelt, MD, USA
[2]Laboratory of Hydraulics, Hydrology and Glaciology (VAW), ETH Zurich, Zurich, Switzerland
[3]Earth System Science Interdisciplinary Center, University of Maryland, College Park, MD, USA

Received: 29 October 2015 – Accepted: 13 November 2015 – Published: 25 November 2015

Correspondence to: C. F. Dow (christine.f.dow@nasa.gov)

Published by Copernicus Publications on behalf of the European Geosciences Union.

Abstract

The growth and drainage of active subglacial lakes in Antarctica has previously been inferred from analysis of ice surface altimetry data. We use a subglacial hydrology model applied to a synthetic Antarctic ice stream to determine internal controls on the filling and drainage of subglacial lakes and their impact on ice stream dynamics. Our model outputs suggest that the highly constricted subglacial environment of the ice stream, combined with relatively high rates of water flow funneled from large catchments, can combine to create a system exhibiting slow-moving pressure waves. Over a period of years, the accumulation of water in the ice stream onset region results in a buildup of pressure creating temporary channels, which then evacuate the excess water. This increased flux of water through the ice stream drives lake growth. As the water body builds up, it too steepens the hydraulic gradient and allows greater flux out of the overdeepened lake basin. Eventually this flux is large enough to create channels that cause the lake to drain. Due to the presence of the channels, the drainage of the lake causes high water pressures around 50 km downstream of the lake rather than immediately in the vicinity of the overdeepening. Following lake drainage, channels again shut down. Lake drainage depends on the internal hydrological development in the wider system and therefore does not directly correspond to a particular water volume or depth. This creates a highly temporally and spatially variable system, which is of interest for assessing the importance of subglacial lakes in ice stream hydrology and dynamics.

1 Introduction

Subglacial lakes store large quantities of water in bedrock overdeepenings and regions of hydraulic convergence underneath the Antarctic ice sheets, including the highly dynamic ice streams (e.g., Wingham et al., 2006; Wright and Siegert, 2012). The role of these water bodies in ice dynamics is largely unknown and limited by availability of data

TCD
9, 6545–6579, 2015

and knowledge of the basal hydrological regimes. The former has been increasingly addressed with satellite surface altimetry data products, allowing analysis of surface ice flexure in the region of subglacial lakes (e.g., Gray et al., 2005; Fricker et al., 2007). It has been found that many of the lakes in regions of fast flowing ice are active over the period of < 1–5 years causing ice uplift and subsidence related to the lake filling and draining (e.g., Fricker et al., 2010). The drainage of lakes have been found, in the case of Byrd Glacier in the East Antarctic, to cause significant downstream ice speed up of over the period of 1–2 years (Stearns et al., 2008). Basal lakes also appear to be hydrologically interconnected as demonstrated by ice subsidence coincident with downstream ice uplift at lakes located 290 km apart in Adventure subglacial trench in the East Antarctic (Wingham et al., 2006).

In situ data of hydrological conditions at the bed of the Antarctic ice sheets are limited due to difficultly of access. As an alternative, numerical models can be used to infer conditions at the ice-bed interface and to estimate the impact of subglacial lakes on hydrological development. To date, hydrological models of Antarctic subglacial lakes have been primarily diagnostic rather than prognostic and rely on ice surface uplift and subsidence data to determine the threshold switch between lake filling and draining (Carter et al., 2009, 2011; Carter and Fricker, 2012). Pattyn (2008) used a synthetic approach with a full Stokes ice flow model to assess triggers for Antarctic lake drainage. Those model outputs suggested that small changes in water input into a lake can cause episodic, although partial, drainage and related changes in the ice surface slope. An ice flow modeling approach was also used by Sergienko et al. (2007) to assess changes in the ice surface slope and local dynamics due to lake drainage. That study found that changes in lake depth are not directly translated to ice surface uplift and subsidence so that assessing lake volume from ice surface altimetry is challenging. These ice dynamics models begin to address the feedbacks between ice flow and subglacial lake filling and drainage, but did not include an active hydrological network, necessary to determine the larger, catchment-scale causes of lake stability.

TCD
9, 6545–6579, 2015

Here we present the first application of a 2-D basal hydrology model to analyze subglacial Antarctic lake stability and the impact of drainage on ice stream hydrological development and dynamics. We use GlaDS, a finite-element hydrological model, which incorporates both distributed and efficient drainage components. It has previously been applied to simulate drainage systems of synthetic ice sheet catchments and real Alpine glaciers (Werder et al., 2013). We apply this model to a synthetic regime in Antarctica, designed to emulate Recovery Ice Stream, a region with up to thirteen active lakes (Fricker et al., 2014), to assess the behavior and stability of subglacial lakes in the Antarctic. Our approach is novel as it does not require any external forcing to fill and drain the lakes (cf. Carter and Fricker, 2012), which instead occurs due to internal model dynamics.

2 GlaDS model

GlaDS (Glacier Drainage System model) is a 2-D finite element model that incorporates equations for subglacial R-channel growth and linked cavity system development. The model configuration and application to synthetic ice sheet catchments and valley glacier systems is described fully in Werder et al. (2013); here we give a brief overview of the model. The effective pressure, N, in the system is

$$N = p_\mathrm{i} - p_\mathrm{w}, \tag{1}$$

where p_w is the water pressure and $p_\mathrm{i} = \rho_\mathrm{i} g H$ is the ice overburden pressure with ρ_i the ice density, g the gravitational acceleration, and H the ice thickness. Mass conservation in the distributed linked-cavity system is described with

$$\frac{\partial h}{\partial t} + \frac{\partial h_\mathrm{e}}{\partial t} + \nabla \cdot q = m, \tag{2}$$

where h is the average thickness of the water layer, h_e is an effective storage layer thickness representing either an englacial or basal sediment aquifer, q is the water discharge and m is the prescribed source term for the distributed system representing, in

TCD
9, 6545–6579, 2015

this case, geothermal and frictional basal melt. Change in the water thickness is determined by cavity opening from sliding over basal bumps and closing through viscous ice deformation. Flux in the distributed system is related to gradients in hydraulic potential, $\phi = \rho_w g B + p_w$, where ρ_w is the water density and B is the bed elevation. Channels are modeled as semi-circular R-channels that grow due to melting and close due to viscous creep of ice. Mass conservation in the channels is described with

$$\frac{\partial S}{\partial t} + \frac{\partial Q}{\partial s} = \frac{\Xi - \Pi}{\rho_w L} + m_c, \quad (3)$$

where S is the channel cross-sectional area, Q is the discharge through the channel, s is the horizontal distance along the channel, Ξ is the dissipation of potential energy, Π represents the change in sensible heat, L is the latent heat of fusion and m_c is the water that enters the channel from the surrounding distributed system. Model parameters are given in Table 1 and follow the same nomenclature as in Werder et al. (2013).

The model mesh is unstructured with channels calculated along the element edges to form a network. Water is exchanged between channel segments at the element nodes. The distributed system is calculated within and across the elements. Interaction between the two hydrological systems is determined by assuming the water pressure is the same in a channel and the distributed sheet immediately adjacent to it. Crucially for our application to subglacial lake development, the pressure calculated in the distributed system also includes the water thickness so that a body of water, such as a lake, will have a direct impact on the system hydraulic potential.

3 Model configuration

We configure GlaDS to represent a synthetic Antarctic system with characteristics similar to Recovery Ice Stream in the East Antarctic ice sheet. Recovery Ice Stream has been identified to have up to 13 active lakes that periodically fill and drain (Fricker et al., 2014). This system also has one of the largest catchments in the East Antarctic, draining 8 % of the ice volume (Joughin et al., 2006), and is of considerable interest for analysis of lake drainage dynamics (Bell et al., 2007; Langley et al., 2011, 2014; Fricker et al., 2014). Our synthetic system is a simplified version of the Recovery region with a domain featuring a large catchment of area 5.4×10^5 km^2 feeding into an ice stream of width 50 km and length 300 km (see Fig. 1). The total area of the upper catchment equals the Recovery subglacial drainage catchment area feeding into the ice stream, calculated using routing algorithms assuming water is at ice overburden pressure, applied to the BEDMAP2 basal and surface digital elevation models (DEMs) (Fretwell et al., 2013).

Two topographies are used within the model domain. The first has a planar basal slope of 0.06°. Due to the shallowing of ice surface slopes in the interior of Antarctic ice stream catchments, we construct a steeper surface slope of 0.29° in the ice stream and 0.11° in the catchment. This gives a maximum ice thickness of 3337 m. The second topography is identical to the first one except for an added overdeepening located 150 km upstream from the lower boundary. This overdeepening is created using a Gaussian formulation with a fixed radius of 7.5 km and maximum depth of 150 m overlain onto the basal planar slope.

Water input to the distributed system is continuous across the domain, representing water production from both geothermal and frictional heating. Initially, we apply an input rate of 0.5 mm a^{-1}, a level that is likely too low for the Recovery region, which is used to run the model to steady state. The second scenario uses the predicted water production rate for the Recovery catchment of 1 mm a^{-1} (Fricker et al., 2014). The model is ramped from steady state to this level of water input over the period of 10 years, inducing a gradual change. In these model runs, the channel system has no direct input and channels are initiated from distributed-based flux, i.e., no pre-existing channels are assumed at the beginning of the model runs.

The upper and lateral boundary conditions are Neumann conditions set to zero inflow. The downstream boundary has a Dirichlet pressure condition set at ice overbur-

TCD
9, 6545–6579, 2015

den pressure to represent the ocean outlet of Recovery Ice Stream. Tidal influences on marginal water pressure are not included in this model set-up.

Our standard model parameters are listed in Table 1. Given lack of knowledge of the basal conditions in many regions of Antarctica, we perform sensitivity experiments to test the applicability of the model and also to assess controls on subglacial lake stability. These sensitivity parameters include tests on the overdeepening size, the conductivity of the distributed system vs. the efficient system, and the volume of water produced at the bed. The variations of these parameters are given in Table 2. For each variation, the model is first allowed to run to steady state.

For the second topography, the model mesh is refined within the overdeepening to allow accurate calculation of changes within the subglacial lake. In these runs, the minimum element edge length is 220 m in the overdeepening and 780 m in the ice stream. These edge lengths increase to an average of 1500 m in the upper catchment.

4 Results and analysis

4.1 Planar bed topography

We begin by examining the hydrological development of the ice stream assuming no overdeepenings and a fully planar bed configuration. The steady state solution for our model with low water production throughout the system causes the model to drop below overburden everywhere, including to 75 % of overburden within the ice stream. This low pressure occurs because there is not enough water to pressurize the distributed cavities for an ice speed of 100 $\mathrm{m\,a^{-1}}$. Antarctic systems likely operate close to overburden pressure due to the substantial ice thickness (Engelhardt and Kamb, 1997) and as a result, this steady state modeled solution is not realistic for the Recovery system.

In the second scenario, the water input rate is gradually increased over 10 years to that predicted for Recovery Ice Stream (i.e., 1 $\mathrm{mm\,a^{-1}}$). The increased flux in the Recovery catchment initiates pressure waves in the ice stream where water is funneled from the large catchment. We define a pressure wave as a ridge of water above ice overburden pressure, which propagates downstream. This is demonstrated in Fig. 2 where the change in effective pressure along the ice stream center line is plotted. In the Recovery system, these pressure waves repeat and by year 70 have settled into a periodic pattern as shown in Fig. 3a and b. This figure plots the average water pressure at locations 200 and 100 km from the margin, along with channel cross-sectional area. In these regions, the channels grow to $\sim 0.3\,\mathrm{m}^2$ and reduce to $< 0.02\,\mathrm{m}^2$ cross-sectional area over a pressure wave cycle. There is therefore a link between the pressure wave and the growth of channels. It appears the pressure waves form because there is not enough hydrological capacity or hydraulic gradient in the ice stream to move water funneled from the large catchment downstream. The pressure of the water therefore increases, alters the hydraulic gradient and enhances downstream flux. This greater flux then encourages growth of channels. Once the pressure wave has passed, flux rates decrease and the channels close.

Figure 3c shows N along the center line for a series of pressure waves moving through the system. The pressure waves have, on average, a speed of $220\,\mathrm{m\,day}^{-1}$ with an area remaining under pressures higher than overburden for up to two years. An example of one pressure cycle from year 85 to 88 is also plotted with the number of days the area is above overburden and the length scale affected by overpressure at that time (Fig. 3d). The longitudinal length affected by pressures above overburden varies on the timing of the wave cycle, increasing to a maximum of ~ 170 km when the highest pressure is centered at a distance of ~ 200 km from the downstream boundary of the ice stream (Fig. 3e). As a result, not all of the ice stream is equally affected by high pressures, both in terms of duration and level of pressure.

4.2 Overdeepened bed topography

We now run the same set of experiments using the bed topography that includes an overdeepening. With the low water input forcing, a steady state solution is reached where the pressure is again entirely below overburden, including in the overdeepening.

TCD
9, 6545–6579, 2015

In this steady state, no lake forms in the overdeepening as the volume of water entering the overdeepening always equals the volume of water exiting. If the pressure in the hydrological system was everywhere at overburden pressure, as is commonly assumed when no hydrological modeling capability is available, all water flow would be directed into the overdeepening and form a lake. However, with a fully coupled hydrology model, the system adapts rapidly so that the pressure conditions in the lake are precisely at the level to allow equal outflow for inflow, with pressures slightly lower on the tip of the reverse slope than in the overdeepening so that there is a positive downstream hydraulic potential gradient despite the adverse slope. As a result, the downstream bedrock ridge does not prevent water flow through the lake.

Using the above steady state as the initial condition and then ramping up the input to the value representative of Recovery Ice Stream again causes pressure waves to occur (Fig. 4). As shown in Fig. 4a and b, the overdeepening slightly changes the timing of pressure waves compared to the planar model runs (see Fig. 3a and b). However the range of pressure change upstream of the overdeepening is similar between the planar and the overdeepening runs.

In the overdeepening, a lake forms when the changing hydraulic gradients induced by the pressure waves prevent adjustment of the hydrological system to the rate of water influx (Fig. 5). As the lake deepens, the hydraulic gradient over the bedrock ridge is steepened and water flux over the ridge is increased. This greater water flux allows channels to form on the downstream tip of the overdeepening and lake drainage occurs when the channels downstream of the lake reach a threshold size. Following lake drainage, water flux over the bedrock ridge slows and the downstream channels close (Fig. 5). The lake begins to form again when upstream hydraulic potential gradients change due to passage of another pressure wave, driving more water into the overdeepening.

Multiple lake drainages occur over the period of 100 years. As shown in Fig. 6, the lake does not always fill to the same volume prior to drainage, and also has a variety of filling and drainage rates. On average, the maximum lake water depth and volume are

1.3 m and 0.86 km^3, respectively. Once the lake has drained, the average lake depth is 0.47 m (Fig. 6a and c). The lake filling times range between ∼ 1–3 years with an average of 1.65 years and drainage times between ∼ 0.8–2.75 years, with an average of 1.8 years. The lake filling and drainage rates peak for each cycle at an average of ∼ 1 and 1.5 $m^3\,s^{-1}$, respectively. The fastest lake drainage rate is 2.3 $m^3\,s^{-1}$ (Fig. 6d). The water pressure ranges between 0.95 and 1.04 as fractions of overburden (or 0.7 and −0.6 MPa effective pressure).

The changes in lake pressure do not always match the timing of lake growth and drainage and instead there is sometimes a pattern of two pressure waves for one lake drainage (Fig. 5). This is characterized by a pause in lake drainage as the pressure wave moves through the system, as shown in the lake depth output in Fig. 5. The initial growth of the lake is driven by movement of the first pressure wave through the system. However, when the second wave moves through, the channels are sufficiently developed in the downstream region of the lake that they have capacity for the additional water driven into and out of the overdeepening. This channel capacity prevents the second pressure wave causing negative effective pressures downstream of the lake (Figs. 4c and 5). The pause in lake drainage is due to a combination of downstream channel pressurization and additional water flowing through the overdeepening. One lake drainage over two pressure wave cycles demonstrates that the pressure waves are not the only cause for lake growth and drainage but instead provide changing hydraulic conditions that prevent a steady state. As shown below in the sensitivity tests, the impact of the pressure wave on the lake growth and drainage timing depend on the conductivity of the system and the volumes of water in the hydrological networks.

Channel growth and shrinkage rates at the downstream margin of the lake are plotted in Fig. 7a along with the lake water level. During lake drainage, channels at the lake margin grow to a size of ∼ 0.07 m^2, although 10 km downstream they temporarily increase to a maximum of 17 m^2 (Fig. 7b). The channels are not always the same size when the lake drainage begins. The main discernible pattern is that lower lake volumes at the end of drainage and smallest channel sizes coincide. Beyond this, the rate of channel growth is also dependent on the pressure gradients downstream of the lake and on downstream channel size. As a result, exact controls for lake drainage timing are difficult to ascertain.

5 Sensitivity results

We tested the impact of overdeepening size on lake growth and drainage (Fig. 8a). We found that, when the overdeepening depth was decreased from 150 to 50 m, very little water accumulated in the basin, with water depths increasing by ~ 8 cm during a growth and drainage cycle. A deeper overdeepening of 250 m caused much greater water accumulation with lake depths up to 6 m. The larger overdeepening also forms and drains slightly more quickly compared to the standard overdeepening of 150 m.

We also adapt the volume of water produced at the bed. When the rate is decreased from 1 to 0.85 mm a^{-1} there is a delay in onset of lake formation (Fig. 8b). Also the depth of the lake is smaller than with the standard melt input at < 1 m. For input rates smaller than 0.85 mm a^{-1}, no lakes form and no pressure waves occur. With water production rate doubled to 2 mm a^{-1}, lake drainages and pressure waves occur more frequently and initiate earlier, although the lake water levels are on a similar range.

Lowering the distributed system conductivity from 1×10^{-3} to 1×10^{-4} $m^{7/4}\,kg^{-1/2}$ causes a deeper lake to form, with lake growth and drainage occurring over a longer time scale (Fig. 8c). When the conductivity is raised slightly to 1.1×10^{-3} $m^{7/4}\,kg^{-1/2}$, the lake takes longer to form than the standard run because the ice stream capacity is larger and therefore it takes more time to achieve near-overburden pressure and induce the pressure waves. With a higher distributed system conductivity, the system remains in steady state, no pressure waves develop, and no lake forms. There is therefore a narrow range of distributed system conductivity where the lake will form and drain. However, combinations of different parameters also allow stable lake growth and drainage. For example, a higher distributed system conductivity with greater water input allows lake formation.

When channel conductivity is lowered from 5×10^{-2} to 5×10^{-3} m$^{3/2}$ kg$^{-1/2}$, no channels form at the margin of the lake and the pressure and lake level remain high throughout the model run (Fig. 8d). With a high channel conductivity of 5×10^{-1} m$^{3/2}$ kg$^{-1/2}$ the system capacity of the ice stream is increased so pressure features do not form, the ice stream is mostly in steady state and a lake does not grow. In this situation, the overdeepening water pressure stabilizes around 96 % of overburden.

6 Discussion

The subglacial systems of Antarctica are regions where little is known about the spatial and temporal evolution of the hydrological systems and their impacts on ice dynamics. With this hydrological modeling exercise we have produced outputs that suggest the system is substantially different from that of the more closely studied mountain, and to some extent, Greenlandic outlet glaciers. In the Antarctic, one of the defining features is that no water is input to the bed from the surface and therefore any variability at the bed is not driven on a seasonal scale but instead over years or even decades. This characteristic causes two major difficulties when attempting to establish how Antarctic basal hydrology develops: (1) the subglacial production of water is based on modeled geothermal heat fluxes and modeled ice fluxes rather than measured water inputs rates from the surface and (2) available data records, particularly from satellite sources, are limited to the last couple of decades. However, by applying a 2-D hydrology model, which produces lake filling and drainage through internal dynamics, we can make a step towards understanding and predicting the complex developments of subglacial Antarctic systems.

6.1 Pressure waves

Greenland and mountain glacier hydrological systems are driven by seasonal water input from the ice surface whereas Antarctic ice streams have no seasonal hydrological signal. The Greenland Ice Sheet and mountain glaciers also receive more than an order of magnitude more water volume from the surface than is produced at the bed of Antarctic ice streams through frictional and geothermal heating. It is therefore to be expected that the hydrological development in these systems is also different. In mountain glaciers, much work has been dedicated to identifying development of efficient drainage networks that cause a decrease in ice velocity following a speed up at the beginning of the melt season when water enters an initially constricted system (e.g., Iken and Bindschadler, 1986; Röthlisberger and Lang, 1987; Schoof, 2010). In Greenland, a similar phenomena has been identified near the ice sheet margin (e.g., Bartholomew et al., 2012; Cowton et al., 2013; Joughin et al., 2013). In the Antarctic, our hydrology model outputs suggest that the funneling of water from a large catchment at the production rate expected for an ice stream like Recovery allows the water in the ice stream to flow continually at pressures close to and sometimes above overburden. Fast flow speeds in ice streams are strong evidence that this situation does occur in reality (e.g., Rignot et al., 2011). The growth of channels in the ice stream does diminish pressures but only to a level of $\sim 0.95 \times P_{\text{i}}$ and therefore are not impacting temporal changes in ice dynamics to the extent observed in mountain glaciers. However, growth of channels are a key driver in allowing movement of the pressure waves.

The pressure waves are an interesting phenomena that have not been a common feature of glacial hydrology models. From our sensitivity tests we find that a combination of factors allow the waves. These are low hydraulic potential gradients due to shallow surface slopes, relatively low water fluxes, and funneling of water from a large catchment so that the water input rate is higher than the capacity of the ice stream. Our hydrological explanation for the waves is that water pressure builds up in the constricted system, followed by faster water flow resulting in temporary channel growth, which moves the excess water downstream. There is therefore a close connection between the rate of pressure change, distributed water thickness and channel growth. Despite this, the water thickness in the cavities only increases by a maximum of 8 cm suggesting that it would be difficult to see such a pressure change in surface elevation data. However, the regions affected by high water pressure could cause an increase in ice velocity that might be identifiable using surface feature tracking methods.

There is evidence from other glacial systems that transient regions of high pressure in constricted systems do arise. Borehole data from Schoof et al. (2014) demonstrate that transient pressure oscillations occur during the winter in a glacier in the Yukon Territory of Canada, driven by low water flux rates in a constricted system. These oscillations lasted over a period of days rather than years, as our model suggests could be occurring in Antarctic ice streams. Schoof et al. (2014) modeled this system on an idealized flowline and demonstrate that storage of water is an important control on the timing of internally-driven oscillations. Given the significant differences between a Yukon mountain glacier and an Antarctic ice stream it is not surprising that system oscillations would occur at different periodicities. However, it is encouraging that field evidence exists of internally driven transience when the basal hydrological system is expected to be highly constricted. Further evidence of pressure waves comes from surging glaciers. Interferometric analysis of the 1995 Bering Glacier surge in Alaska identified numerous "bull-eyes" suggested to represent regions of surface uplift due to high pressure from water in a constricted system (Fatland and Lingle, 2002). This region remained under pressure between 1–3 days as water moved downstream. Similar regions of temporary uplift were also observed on a nearby non-surgetype glacier during the winter months when little water was moving through the system (Lingle and Fatland, 2003). Again, these pressure waves transition much more quickly than we suggest for our Antarctic system but illustrate that such oscillations are observable in data.

6.2 Subglacial lakes

The hydrological model produces lake growth and drainage over a cumulative range of 2–4.5 years (Fig. 6). This cycle is driven by both the pressure waves and the growth of channels downstream of the lake. As such, the lake drains due to similar criteria that characterize jökulhlaups in regions like Grímsvötn, Vatnajökull, in Iceland. The lake water accumulation in the latter type of system is driven by increased melt through volcanically-inducted heating. As the water builds up in the basin, some leakage seeds channel growth (e.g., Nye, 1976; Clarke, 1982). The "seal" preventing lake drainage can be broken when the lake is at positive effective pressures depending on development and pressurization of the system downstream of the lake (Fowler, 1999). The jökulhlaup model of Fowler (1999) is based on there being a region of reverse hydraulic gradient downstream of the lake which migrates upstream as the lake grows and alters the effective pressure gradient. In our modeled subglacial lakes in the Antarctic, the lake pressure is important in that it changes the hydraulic potential gradient driving water over the reverse bedrock slope, but there is no physical "seal" of reverse hydraulic potential gradients. Instead it is a threshold channel size and overall system hydraulic gradient driven by changes further downstream that allow the lake to drain (Fig. 5). The lakes are not draining at the time of maximum pressure in the lake so that, while it is not fully realistic to not take account of ice flexure at times of water overpressure, it is not the overpressure alone that is causing lake drainage (Fig. 6). As shown in Fig. 5, one lake growth and drainage cycle can occur over two pressure waves. This is because the channels are efficient enough by the second pressure wave to conduct the extra water driven into and out of the overdeepening. The second pressure wave therefore dissipates once it reaches the overdeepening and the channels prevent negative effective pressures downstream of the draining lake. The fact that the lake does not grow and drain every time a pressure waves passes is further evidence that the size of channels both immediately downstream of the lake and further downstream in the system (creating the necessary hydraulic gradients) is crucial for both lake growth and drainage. Our sensitivity tests with less conductive channels demonstrates that, without the growth and shrinkage of channels, the lake does not drain (Fig. 8d).

The lack of repeatable cycles of lake growth and drainage is similar to the jökulhlaup cycles modeled by Kingslake (2015). Based on the Nye (1976) equations, that model demonstrated that lake floods driven by different rates of meltwater input had characteristics including chaotic dynamics (where the initial conditions strongly controlled lake flood timing and cycles did not repeat). Our lake filling and draining cycles reveal

TCD
9, 6545–6579, 2015

properties similar to the flood characteristics described by Kingslake (2015). We see situations where meltwater input (driven by the pressure waves) causes a lake growth and drainage closely linked to the wave (see years 65 to 73 in Fig. 6). As described, we also have one lake drainage over two pressure wave cycles. The lake growth and drainage is non-repeating (Fig. 6a) even though, in the scenario without an overdeepening, the pressure wave settles into a stable pattern by 70 years (Fig. 3a and b). As a result, our outputs also suggest chaotic dynamics and demonstrate that this can be a condition of 2-D hydrological networks in addition to 1-D models.

One important characteristic of the subglacial lakes to note is that, at no stage does the overdeepening fully prevent downstream flux of water over the reverse bedrock slope. The presence of a subglacial basin therefore only hampers water flux rather than preventing it. This is because the hydrological system is rarely static at overburden pressure. Instead, when the system approaches overburden the pressure waves cause continual changes in water pressure. At all stages of the model runs, the water can flow up the adverse slope of the overdeepening because the pressures at the tip of the overdeepening can exist slightly below overburden as a result of the small channels. This creates a gradient due to the higher pressures in the lake that allows water to flow up the reverse slope. The relative difference between the pressure in the lake and on the adverse slope tip is a key driver for how much water can exit the lake. In terms of lake dynamics, this process suggests that an instability must be present in the modeled system to allow lake growth and drainage, otherwise the system tends to steady state and no lakes form. In our modeled system the instability is caused by the pressure waves that continually change the hydraulic gradients in the system.

Ice surface elevation data has been available from satellite-based sources such as ICESat. The ice surface altimetry allows identification of lake filling and draining cycles over the period of a decade. The longevity of lake volume change means that it is not yet possible to determine whether the somewhat chaotic nature of lake growth and drainage as demonstrate by the model outputs is also seen in nature. It will require data from ICESat2, due to launch in 2017, to continue the record and assess development of the system over the next couple of decades.

The lake that forms in our overdeepening is meters thick rather than filling the basin of depth 150 m. This has important implications for attempts of calculating Antarctic-wide estimates of water budgets that include active lakes. Carter et al. (2011) and Carter and Fricker (2012) modeled water budgets for the Siple Coast region of the West Antarctic using water flux over an hydropotential surface and lake filling and drainage rates inferred from satellite altimetry data. This approach assumed that all water was flowing at overburden pressure and that overdeepenings prevented downstream water flux as the lakes were filling. Carter and Fricker (2012) adapted their model to allow for "leaking" lakes that did not act as sinks but allowed all water to throughflow. This water budgeting method produced encouraging results linking the satellite altimetry data with estimated basal melt rates. Our model outputs suggest, however, that overdeepenings can allow downstream water flow at the same time as accumulating lakes, and also that varying pressures in the system are very important for lake growth and drainage. This could impact the rates of filling and drainage of the Siple Coast lakes examined by Carter et al. (2011) and Carter and Fricker (2012), and perhaps constrain some of the discrepancies between modeled lake filling and drainage rate when compared with the altimetry inferred rates.

Changes of lake water level in the range of meters is also consistent with the rates of ice surface uplift observed from altimetry measurements at Recovery Ice Stream (Fricker et al., 2014). Our lake area is 177 km^2 and located 150 km from the ice margin. It is therefore somewhat comparable to lakes 4 and 5 in Recovery Ice Stream (although these are both slightly larger in area at 220 and 273 km^2, respectively, Fricker et al., 2014). Recovery lake 3 is 50 km downstream and is smaller with an area of 60 km^2. It is difficult to compare our model results directly with the Recovery system because the latter is made up of many lakes and complex topography. However, cumulatively lakes 4 and 5 were suggested to have increased by 0.33 km^3 over four years. These then drained by 0.22 km^3 at a rate of 3.7 m^3 s^{-1}. In contrast, lake 3 drained by 0.07 km^3

TCD
9, 6545–6579, 2015

with a flux rate of 0.57 $m^3 s^{-1}$ over less than two years (Fricker et al., 2014). Our typical model outputs for an overdeepening of area 177 km^2 with a depth of 150 m, has lake growth of $\sim$ 0.05 km^3 over 1.6 years at a rate of $\sim$ 1 $m^3 s^{-1}$ and drainage over two years at a maximum rate of 1.5 $m^3 s^{-1}$. As a result, our model outputs lie somewhere in between the larger and smaller Recovery lakes and gives us confidence in our results.

6.3 Impact on ice dynamics

Due to the growth of channels during subglacial lake drainage, there are rarely negative effective pressures directly downstream of the lake at the time of drainage. Instead, the channel are of sufficient size that they move the higher pressure water to around 50 km downstream of the lake. However, due to the pressure waves moving through the entire ice stream there are occasions during lake growth when effective pressures are negative around the region of the lake, contributing to channel development on the tip of the reverse bedrock slope (Fig. 3). As a result, there is a complex dynamical signal that is related more closely to the pressure waves than the lake drainage. This could be challenging to identify in ice surface velocity records although, given that few high temporal resolution velocity calculations have been made for areas like Recovery Ice Stream, it is possible that similar high pressure features have not yet been identified.

The growth and shrinkage of channels in mountain glacier and Greenlandic systems have been directly connected to changes in ice velocity (e.g., Iken and Bindschadler, 1986; Bartholomew et al., 2012). These channels are argued to form only during the summer melt-season and persist for several months before shutting down over winter. In our modeled Antarctic system, however, channels can persist for a number of years and can obtain large sizes. The largest channel in the run with no lake grows from 0.7–19.1 m^2 over four years and then collapses back to 0.2 m^2 in less than a year. The faster shrinking rate compared to channel growth is a result of the thick ice causing rapid creep into the channel once pressures drop below overburden. This is an extreme example of a temporary channel in the modeled system. Instead most channels grow to $\sim 0.4\,m^2$ as the pressure wave transitions through the region. Although basal water is not produced in great volumes in these Antarctic systems, it is funneled from very large catchments into narrow ice streams and therefore provides a constant supply of water that over many years can cause channel growth. Basal catchments in Greenland are, on the other hand, at least an order of magnitude smaller and therefore water flux during the winter months in these systems will be lower. Also in Greenland, the influx of much higher volumes of water in the summer melt season overwhelms any background hydrological system creating a more temporally dynamic system so that the situation of constant water supply allowing system development is limited to a time period of less than a year.

The persistence of channels over a period of years in Antarctic ice streams may have impacts on basal erosion, particularly on the downstream side of lakes. It is possible that channels can be eroded into the bedrock or into basal sediment. Modeling these processes is beyond the scope of the current project but would be an interesting system to examine further.

6.4 Model limitations

Our modeled synthetic system has limitations in that it is a simplified, for instance, it does not incorporate variable topography, spatially varying basal melt rates or variable basal sliding parameters. However the aim with this model is to gain insight into lake filling and draining characteristics without complicating the system. Including topography in the model could impact the pressure waves and therefore the rates of lake filling and draining. We also assume that water flows through a linked cavity system rather than a sediment based system, with the latter possibly being more prevalent in Antarctic ice streams. Water flux in sediments could be more restricted than in linked cavity systems. However, it is plausible that sediment-based systems have similar dynamics as linked-cavity networks with sliding opening spaces between the ice and substrate and ice creep closing the space when water pressures drop (Creyts and Schoof, 2009).

We have carefully conducted a series of tests to rule out, as far as possible, that the pressure wave features are numerical artifacts. We have performed tests to check that there is sufficient mesh convergence both in the planar and overdeepened topographies and find similar outputs as Werder et al. (2013) with errors in mean effective pressure and distributed water thickness on the range of 10^{-5} relative to a smaller mesh. The tolerances of the ordinary differential equation solver were also tested and selected accordingly.

Although likely not numerically induced, it is possible the pressure waves are not physical. The water pressures in the model do not exceed $1.04 \times P_\mathrm{i}$ (or $N = -0.5\,\mathrm{MPa}$) and are therefore not unreasonable. However, pressures above overburden can persist in one area for up to two years, which is a long period of overpressure. Including ice dynamics in the model might change the characteristics of the pressure waves. Feedbacks through faster ice flow and coincident cavity opening could allow greater water flux downstream and reduction of water pressure, as is seen by Hewitt (2013). Ice physics such as those included in the models of Pattyn (2008) and Sergienko et al. (2007) where changing ice flux and ice surface slopes can influence lake drainage timing are also not incorporated into our hydrological model. It is therefore likely that more accurate predictions of lake filling and drainage require coupling of hydrology with dynamics models.

Including ice flexure and uplift could also impact the pressure waves and the rate of lake formation. For example, ice uplift at higher pressures could allow flux of water downstream more rapidly than seen in the model and perhaps a reduction in local overpressure. However, it is unlikely that flexure would entirely remove the pressure waves but might instead change the downstream speed of the wave. Future numerical experiments including ice flexure would provide insight into the likely persistence of the pressure waves observed in this hydrological model and the links between lake formation and the surface ice motion observed through satellite altimetry (e.g., Fricker et al., 2010).

Despite the limitations of the current model configuration, this is the first 2-D hydrological model to be applied to Antarctic subglacial lakes, which can produce lake drainage cycles through only internal dynamics. The outputs therefore provide new insights related to hydrological development and subglacial lake dynamics in Antarctic ice streams.

7 Conclusion

We have presented a 2-D model of Antarctic subglacial hydrology development with analysis focused on the growth and drainage of a subglacial lake. The simulation uses a synthetic setup designed to represent a simplified Recovery Ice Stream and catchment with one overdeepening. The hydrological model incorporates both distributed and efficient networks that develop internally.

Due to water influx from a large catchment into the relatively narrow ice stream, the system does not remain in steady state and instead pressure waves develop. Increases in pressure cause steepening of the hydraulic gradient, enhanced downstream flux, and growth of channels as the wave moves downstream. The speed of the pressure waves is $\sim 220\,\mathrm{m\,day^{-1}}$. Following passage of the pressure ridge, the channels shut down due to lack of water flux and pressures drop to levels slightly below overburden. Pressures can exist at these levels even in areas of thick ice because of the fast ice speed in the ice stream ($100\,\mathrm{m\,a^{-1}}$ in our model runs) continually opening basal cavities.

Our model also reproduces lake growth and drainage over similar scales as observed in Antarctic ice streams. Flux out of the lake is possible at all times due to sufficiently steep hydraulic potential gradients, although full lake drainage only occurs when channels on the adverse slope become large enough to funnel the majority of the water from the overdeepening. Channels grow due to a combination of slow flux out of the lake and the pressure waves, although lake drainage is not always tied to the timing of the pressure waves.

TCD
9, 6545–6579, 2015

The results from this synthetic ice stream hydrological experiment suggest that the Antarctic basal systems can be highly transient and variable with interactions between water pressure and channel growth that occur over a scale of years. These results encourage greater data collection of Antarctic ice stream velocities to examine multi-year flux changes and pressure waves.

Acknowledgements. C. F. Dow was supported with a NASA Postdoctoral Program fellowship at the Goddard Space Flight Center, administered by Oak Ridge Associated Universities through a contract with NASA. R. T. Walker was funded by NASA grant NNX12AD03A. S. Nowicki acknowledges the support of the NASA Cryosphere Program.

References

Bartholomew, I., Nienow, P., Sole, A., Mair, D., Cowton, T., and King, M. A.: Short-term variability in Greenland Ice Sheet motion forced by time-varying meltwater drainage: implications for the relationship between subglacial drainage system behavior and ice velocity, J. Geophys. Res., 117, F03002, doi:10.1029/2011JF002220, 2012. 6557, 6562

Bell, R. E., Studinger, M., Shuman, C. A., Fahnestock, M. A., and Joughin, I.: Large subglacial lakes in East Antarctica at the onset of fast-flowing ice streams, Nature, 445, 904–907, 2007. 6550

Carter, S. and Fricker, H.: The supply of subglacial meltwater to the grounding line of the Siple Coast, West Antarctica, Ann. Glaciol., 53, 267–280, 2012. 6547, 6548, 6561

Carter, S. P., Blankenship, D. D., Young, D. A., Peters, M. E., Holt, J. W., and Siegert, M. J.: Dynamic distributed drainage implied by the flow evolution of the 1996–1998 Adventure Trench subglacial lake discharge, Earth Planet. Sc. Lett., 283, 24–37, 2009. 6547

Carter, S. P., Fricker, H. A., Blankenship, D. D., Johnson, J. V., Lipscomb, W. H., Price, S. F., and Young, D. A.: Modeling 5 years of subglacial lake activity in the MacAyeal Ice Stream (Antarctica) catchment through assimilation of ICESat laser altimetry, J. Glaciol., 57, 1098–1112, 2011. 6547, 6561

Clarke, G. K. C.: Glacier outburst floods from 'Hazard Lake' Yukon Territory, and the problem of flood magnitude prediction, J. Glaciol., 28, 3–21, 1982. 6559

Cowton, T., Nienow, P., Sole, A., Wadham, J., Lis, G., Bartholomew, I., Mair, D., and Chandler, D.: Evolution of drainage system morphology at a land-terminating Greenlandic outlet glacier, J. Geophys. Res.-Earth, 118, 29–41, 2013. 6557

Creyts, T. T. and Schoof, C. G.: Drainage through subglacial water sheets, J. Geophys. Res.-Earth, 114, F04008, doi:10.1029/2008JF001215, 2009. 6563

Engelhardt, H. and Kamb, B.: Basal hydraulic system of a West Antarctic ice stream: constraints from borehole observations, J. Glaciol., 43, 207–230, 1997. 6551

Fatland, D. R. and Lingle, C. S.: InSAR observations of the 1993–95 Bering Glacier (Alaska, USA) surge and a surge hypothesis, J. Glaciol., 48, 439–451, 2002. 6558

Fowler, A.: Breaking the seal at Grímsvötn, Iceland, J. Glaciol., 45, 506–516, 1999. 6559

Fretwell, P., Pritchard, H. D., Vaughan, D. G., Bamber, J. L., Barrand, N. E., Bell, R., Bianchi, C., Bingham, R. G., Blankenship, D. D., Casassa, G., Catania, G., Callens, D., Conway, H., Cook, A. J., Corr, H. F. J., Damaske, D., Damm, V., Ferraccioli, F., Forsberg, R., Fujita, S., Gim, Y., Gogineni, P., Griggs, J. A., Hindmarsh, R. C. A., Holmlund, P., Holt, J. W., Jacobel, R. W., Jenkins, A., Jokat, W., Jordan, T., King, E. C., Kohler, J., Krabill, W., Riger-Kusk, M., Langley, K. A., Leitchenkov, G., Leuschen, C., Luyendyk, B. P., Matsuoka, K., Mouginot, J., Nitsche, F. O., Nogi, Y., Nost, O. A., Popov, S. V., Rignot, E., Rippin, D. M., Rivera, A., Roberts, J., Ross, N., Siegert, M. J., Smith, A. M., Steinhage, D., Studinger, M., Sun, B., Tinto, B. K., Welch, B. C., Wilson, D., Young, D. A., Xiangbin, C., and Zirizzotti, A.: Bedmap2: improved ice bed, surface and thickness datasets for Antarctica, The Cryosphere, 7, 375–393, doi:10.5194/tc-7-375-2013, 2013. 6550

Fricker, H. A., Scambos, T., Bindschadler, R., and Padman, L.: An active subglacial water system in West Antarctica mapped from space, Science, 315, 1544–1548, 2007. 6547

Fricker, H. A., Scambos, T., Carter, S., Davis, C., Haran, T., and Joughin, I.: Synthesizing multiple remote-sensing techniques for subglacial hydrologic mapping: application to a lake system beneath MacAyeal Ice Stream, West Antarctica, J. Glaciol., 56, 187–199, 2010. 6547, 6564

Fricker, H. A., Carter, S. P., Bell, R. E., and Scambos, T.: Active lakes of Recovery Ice Stream, East Antarctica: a bedrock-controlled subglacial hydrological system, J. Glaciol., 60, 1015–1030, 2014. 6548, 6549, 6550, 6561, 6562

Gray, L., Joughin, I., Tulaczyk, S., Spikes, V. B., Bindschadler, R., and Jezek, K.: Evidence for subglacial water transport in the West Antarctic Ice Sheet through three-dimensional satellite radar interferometry, Geophys. Res. Lett., 32, L03501, doi:10.1029/2004GL021387, 2005. 6547

Hewitt, I. J.: Seasonal changes in ice sheet motion due to melt water lubrication, Earth Planet. Sc. Lett., 371, 16–25, 2013. 6564

Iken, A. and Bindschadler, R. A.: Combined measurements of subglacial water pressure and surface velocity of Findelengletscher, Switzerland: conclusions about drainage system and sliding mechanism, J. Glaciol., 32, 101–119, 1986. 6557, 6562

Joughin, I., Bamber, J. L., Scambos, T., Tulaczyk, S., Fahnestock, M., and MacAyeal, D. R.: Integrating satellite observations with modelling: basal shear stress of the Filcher-Ronne ice streams, Antarctica, Philos. T. Roy. Soc. A, 364, 1795–1814, 2006. 6550

Joughin, I., Das, S. B., Flowers, G. E., Behn, M. D., Alley, R. B., King, M. A., Smith, B. E., Bamber, J. L., van den Broeke, M. R., and van Angelen, J. H.: Influence of ice-sheet geometry and supraglacial lakes on seasonal ice-flow variability, The Cryosphere, 7, 1185–1192, doi:10.5194/tc-7-1185-2013, 2013. 6557

Kingslake, J.: Chaotic dynamics of a glaciohydraulic model, J. Glaciol., 61, 493–502, 2015. 6559, 6560

Langley, K., Kohler, J., Matsuoka, K., Sinisalo, A., Scambos, T., Neumann, T., Muto, A., Winther, J.-G., and Albert, M.: Recovery Lakes, East Antarctica: radar assessment of subglacial water extent, Geophys. Res. Lett., 38, L05501, doi:10.1029/2010GL046094, 2011. 6550

Langley, K., Tinto, K., Block, A., Bell, R., Kohler, J., and Scambos, T.: Onset of fast ice flow in Recovery Ice Stream, East Antarctica: a comparison of potential causes, J. Glaciol., 60, 1007–1014, 2014. 6550

Lingle, C. S. and Fatland, D. R.: Does englacial water storage drive temperate glacier surges?, Ann. Glaciol., 36, 14–20, 2003. 6558

Nye, J. F.: Water flow in glaciers: jökulhlaups, tunnels and veins, J. Glaciol., 17, 181–207, 1976. 6559

Pattyn, F.: Investigating the stability of subglacial lakes with a full Stokes ice-sheet model, J. Glaciol., 54, 353–361, 2008. 6547, 6564

Rignot, E., Mouginot, J., and Scheuchl, B.: Ice flow of the Antarctic ice sheet, Science, 333, 1427–1430, 2011. 6557

Röthlisberger, H. and Lang, H.: Glacial hydrology, in: Glacio-Fluvial Sediment Transfer: an Alpine Perspective, John Wiley and Sons, New York, 207–284, 1987. 6557

Schoof, C.: Ice-sheet acceleration driven by melt supply variability, Nature, 468, 803–806, 2010. 6557

Schoof, C., Rada, C. A, Wilson, N. J., Flowers, G. E., and Haseloff, M.: Oscillatory subglacial drainage in the absence of surface melt, The Cryosphere, 8, 959–976, doi:10.5194/tc-8-959-2014, 2014. 6558

Sergienko, O., MacAyeal, D., and Bindschadler, R.: Causes of sudden, short-term changes in ice-stream surface elevation, Geophys. Res. Lett., 34, L22503, doi:10.1029/2007GL031775, 2007. 6547, 6564

Stearns, L. A., Smith, B. E., and Hamilton, G. S.: Increased flow speed on a large East Antarctic outlet glacier caused by subglacial floods, Nat. Geosci., 1, 827–831, 2008. 6547

Werder, M. A., Hewitt, I. J., Schoof, C. G., and Flowers, G. E.: Modeling channelized and distributed subglacial drainage in two dimensions, J. Geophys. Res.-Earth, 118, 2140–2158, 2013. 6548, 6549, 6564

Wingham, D. J., Siegert, M. J., Shepherd, A., and Muir, A. S.: Rapid discharge connects Antarctic subglacial lakes, Nature, 440, 1033–1036, 2006. 6546, 6547

Wright, A. and Siegert, M.: A fourth inventory of Antarctic subglacial lakes, Antarct. Sci., 24, 659–664, 2012. 6546

TCD
9, 6545–6579, 2015
Antarctic subglacial lake dynamics
C. F. Dow et al.

Table 1. Model parameters.

Parameter	Symbol	Value	Units
Ice flow constant	A	2.5×10^{-25}	$\mathrm{Pa}^{n}\,\mathrm{s}^{-1}$
Englacial void ratio	e_{v}	10^{-5}	
Gravitational acceleration	g	9.81	$\mathrm{m\,s^{-2}}$
Bedrock bump height	h_{r}	0.08	m
Latent heat of fusion	L	3.34×10^{5}	$\mathrm{J\,kg^{-1}}$
Sheet width below channel	l_{c}	2	m
Cavity spacing	l_{r}	2	m
Glen's flow constant	n	3	
Basal sliding speed	u_{b}	100	$\mathrm{m\,a^{-1}}$
Ice density	ρ_{i}	910	$\mathrm{kg\,m^{-3}}$
Water density	ρ_{w}	1000	$\mathrm{kg\,m^{-3}}$

Table 2. Sensitivity test variables.

Parameter	Symbol	Base value	Variations	Units
Overdeepening depth	D	150	50, 250	m
Sheet conductivity	k	1×10^{-3}	1×10^{-4}, 1.1×10^{-3}	$m^{7/4}\,kg^{-1/2}$
Channel conductivity	k_c	5×10^{-2}	5×10^{-1}, 5×10^{-3}	$m^{3/2}\,kg^{-1/2}$
Sheet input	M	1	0.85, 2	$mm\,a^{-1}$

TCD
9, 6545–6579, 2015
Antarctic subglacial lake dynamics
C. F. Dow et al.

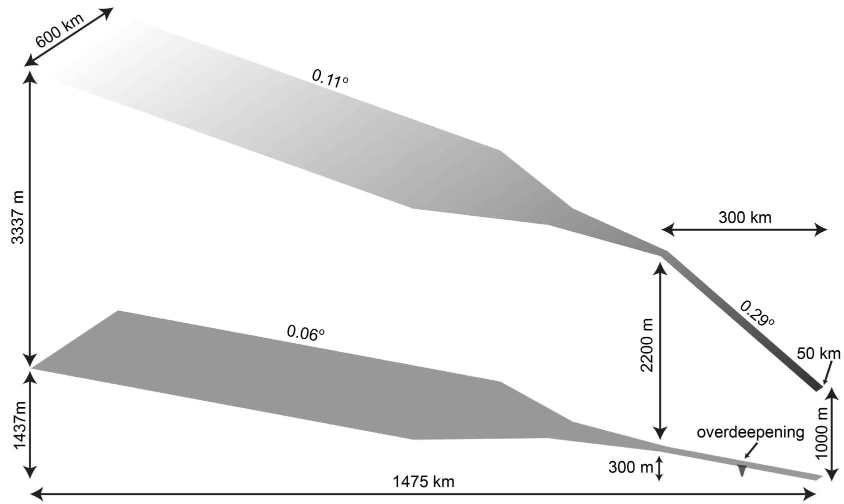

Figure 1. Model domain designed to emulate the catchment of Recovery Ice Stream. The overdeepening has a depth of 150 m. The slopes of the planar surfaces are noted with a steeper surface slope in the narrow ice stream portion of the domain.

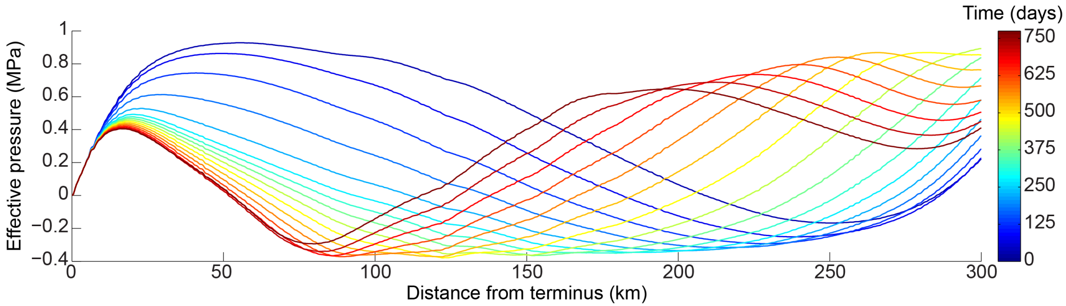

Figure 2. Effective pressure plotted for the ice stream in 50 day intervals, illustrating downstream movement of pressure waves. The outputs range from year 81 to year 83.

TCD
9, 6545–6579, 2015

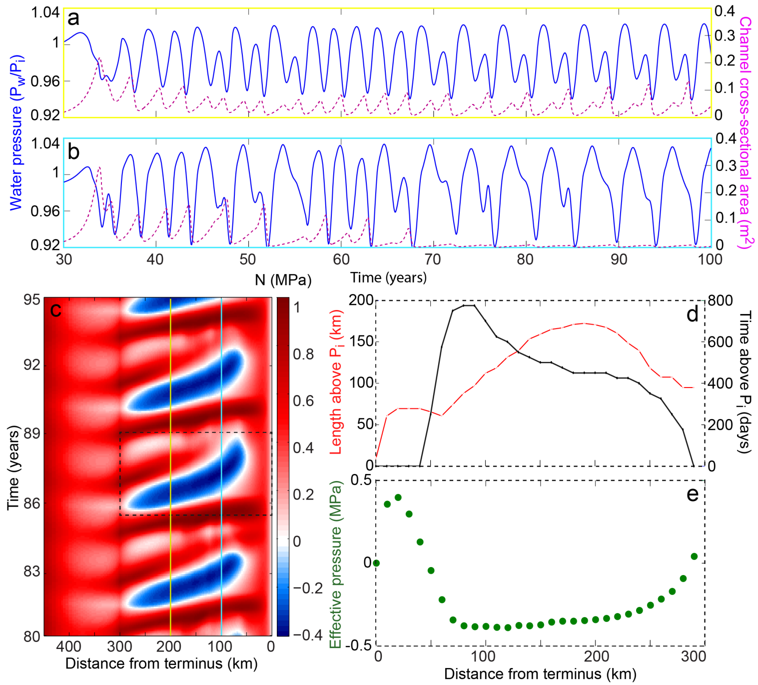

Figure 3. Model outputs from the system with no overdeepening. **(a)** and **(b)** Average water pressure (blue) and channel cross-sectional area (purple dashed) across the ice stream at a distance of 200 and 100 km from the front, corresponding to the colored bars in **(c)**. Prior to 30 years no pressure waves occur and so that time period is not plotted. **(c)** Time-distance plot of center line effective pressure demonstrating several pressure waves. The dashed box shows the feature analyzed in **(d)** and **(e)**. **(d)** Longitudinal length affected by negative effective pressures at the time of pressure wave passing (red curve) and the time of an area with negative effective pressure (black curve) along the ice stream. **(e)** Minimum effective pressure (green) along the ice stream.

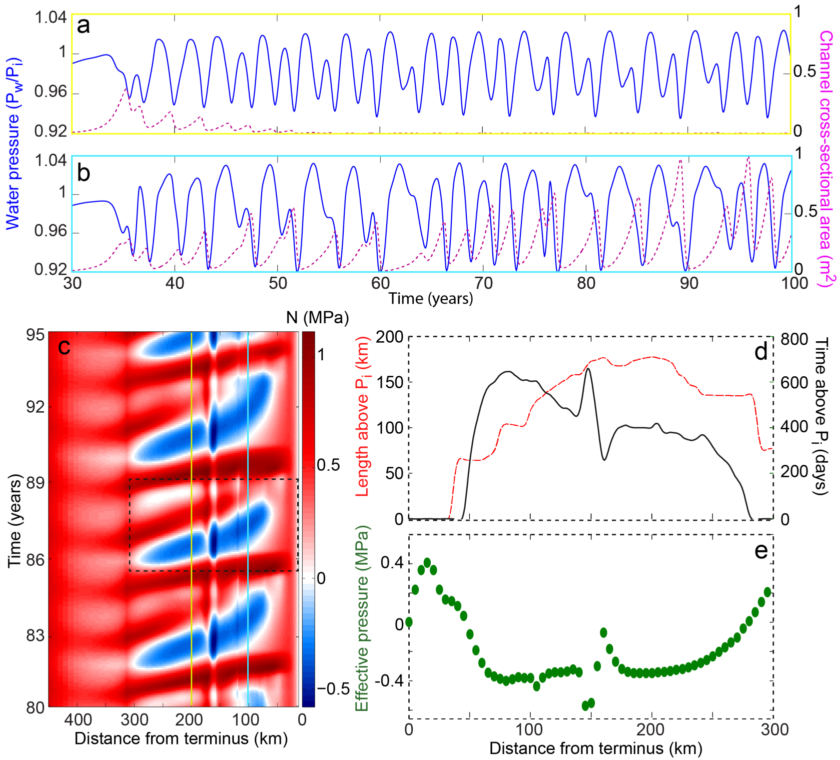

Figure 4. Model outputs from the system with the overdeepening. **(a)** and **(b)** Average water pressure (blue) and channel cross-sectional area (purple dashed) across the ice stream at a distance of 200 and 100 km from the front, corresponding to the colored bars in **(e)**. **(c)** Time-distance plot of center line effective pressure demonstrating several pressure waves. The dashed box shows the feature analyzed in **(d)** and **(e)**. **(d)** Longitudinal length affected by negative effective pressures at the time of pressure wave passing (red curve) and the time of an area with negative effective pressure (black curve) along the ice stream. **(e)** Minimum effective pressure (green) along the ice stream.

TCD
9, 6545–6579, 2015
Antarctic subglacial lake dynamics
C. F. Dow et al.

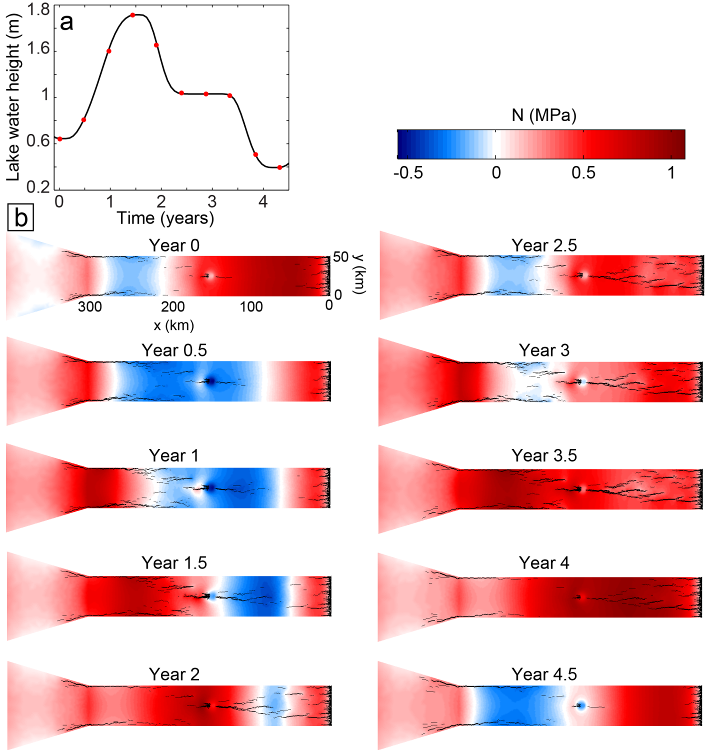

Figure 5. Changes in effective pressure in the ice stream (from years 48 to 52.5) over one lake filling and draining cycle, which occurs over two pressure wave cycles. **(a)** Lake water level (black curve) with pressure plot timing indicated by the red dots. **(b)** Pressure plots at six month intervals. Black lines indicate channels, with the line thickness illustrating channel size. The overdeepening is located 150 km from the terminus.

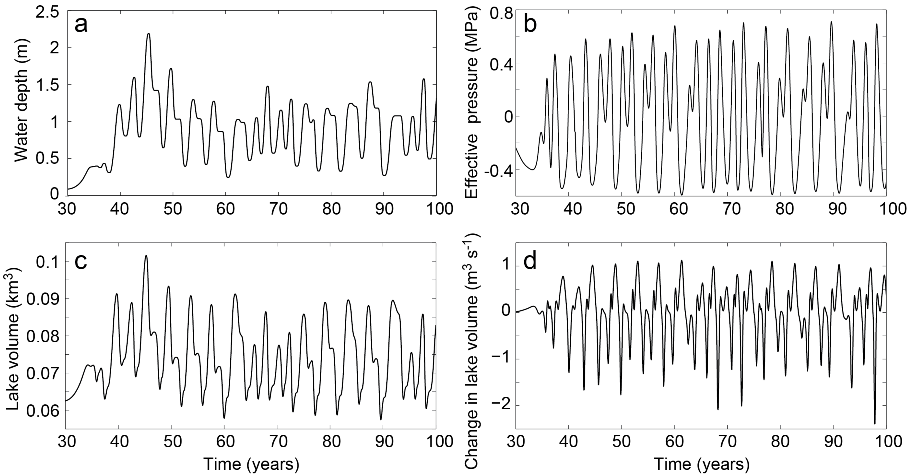

Figure 6. Conditions in the overdeepening over 100 years with **(a)** the maximum lake water depth, **(b)** the water effective pressure, **(c)** the volume of the lake in the overdeepening and **(d)** the filling (positive) and drainage (negative) rates of the lake.

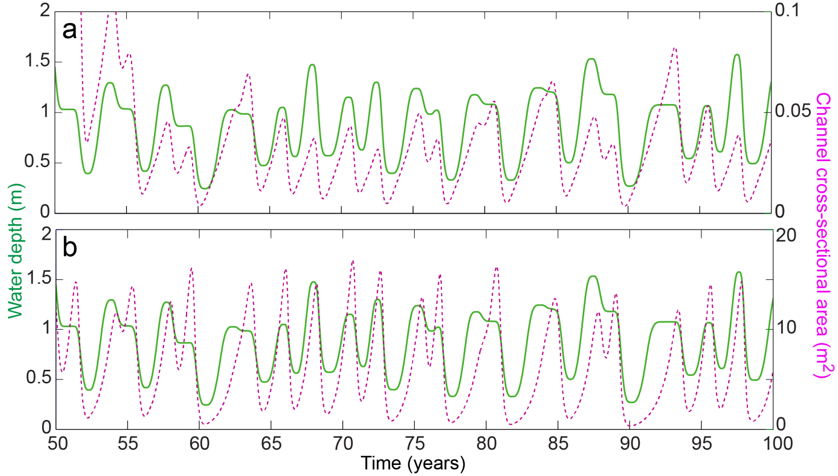

Figure 7. Maximum lake depth (green) and conduit cross-sectional area (purple dashed) at **(a)** the tip of the overdeepening adverse slope and **(b)** 10 km downstream from the overdeepening tip, over 50 years. Lake depth is the same in each plot for direct comparison with channel size.

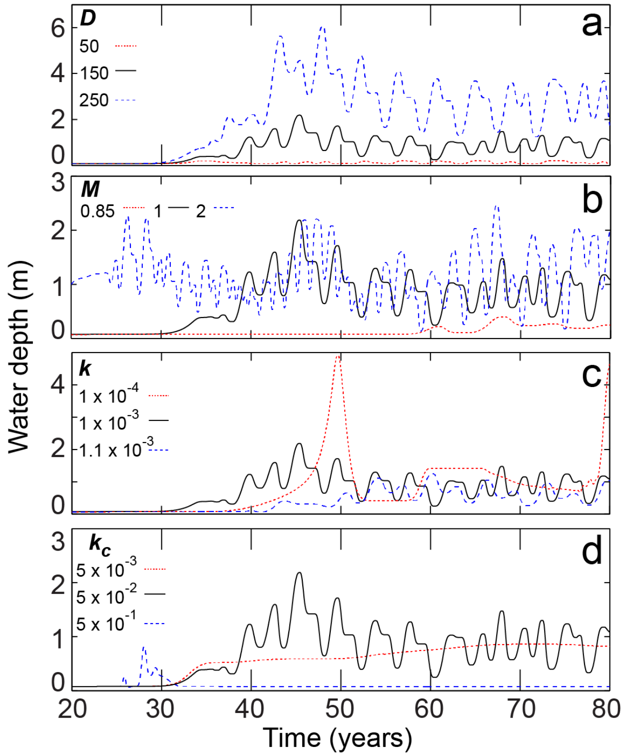

Figure 8. Maximum lake depth in the overdeepening from sensitivity testing. In each plot the black (solid) curve is the standard output. Tests of **(a)** overdeepening depth, D (m), **(b)** water input into the distributed system, M (mm a^{-1}), **(c)** distributed system conductivity k (m$^{7/4}$ kg$^{-1/2}$) and, **(d)** channel conductivity, k_c (m$^{3/2}$ kg$^{-1/2}$).